音明瞭度の測定, 第１１１回日本耳鼻咽喉科学会総会, 仙台市, (2010)
山下哲範, 西村忠己, 岡安　唯, 阪口剛史, 細井裕司, 長谷芳樹, 視覚情報が骨導超音波を用いた補聴システムの語音聴力に与える影響, 第３１３回日耳鼻大阪地方連合会, 大阪, (2010)
岡安　唯, 西村忠己, 山下哲範, 細井裕司, 当科における放射線化学療法によるシスプラチン難聴の評価, 第３１３回日耳鼻大阪地方連合会, 大阪, (2010)
Hosoi Hiroshi, Yanai Syuuichi, Nishimura Tadashi, Sakaguchi Takefumi, Iwakuma T, Yoshino K, Development of cartilage conduction hearing aid, The Eighteenth Inernational Scientific Conference on AMME 2010, Zakopane, (2010)
岡安　唯, 西村忠己, 細井裕司, 年齢と語音明瞭度曲線の傾きについての検討, 第４回聴覚アンチエイジング研究会, 東京, (2010)
福田芙美, 柳井修一, 西村忠己, 清水直樹, 細井裕司, 軟骨伝導によるラット聴性脳幹反応の測定, 日本音響学会聴覚研究会, 三原市, (2010)
Saruwatari Hiroshi, Go Masanobu, Okamoto Ryoi, Shikano Kiyohiro, Hosoi Hiroshi , Binaural hearing aid using sound-localization-preserved MMSE STSA estimator with ICA-based noise estimation, International Workshop on Acoustic Echo and Noise Control (IWAENC2010), Israel, (2010)
下倉良太, 高木悠哉, 西村忠己, 細井裕司, 軟骨伝導振動子の物理特性, 第３１４回日耳鼻大阪地方連合会, 大阪, (2010)
高木悠哉, 下倉良太, 西村忠己, 細井裕司, 住宅内透過騒音尺度作成の試み（1）, 第３１４回日耳鼻大阪地方連合会, 大阪, (2010)
Yamashita Akinori, Nishimura Tadashi, Nagatani Yoshiki, Sakaguchi Takefumi, Okayasu Tadao, Hosoi Hiroshi, Differences between bone-conducted ultrasound and audible sound in speech recognition, The 13th JAPAN-KOREA Joint Meeting of Otolaryngology-Head and Neck , Seoul, (2010)
Okayasu Tadao, Nishimura Tadashi, Yamashita Akinori, Nakagawa Seiji, Yanai Shuichi, Uratani Yuka, Nagatani Yoshiaki, Hosoi Hiroshi, Growth of N1m for stimulus suration through bone-conducted ultrasound modulated by Japanese vowel sound, The 13th JAPAN-KOREA Joint Meeting of Otolaryngology-Head and Neck , Seoul, (2010)
柳井修一, 福田芙美, 西村忠己, 清水直樹, 細井裕司, 軟骨導振動子を用いたラット聴性脳幹反応の測定, 日本心理学会第７４回大会, 豊中市, (2010)
西村忠己, 福田芙美, 斉藤　修, 岡安　唯, 宮前了輔, 下倉良太, 高木悠哉, 細井裕司, 軟骨伝導補聴器の開発－臨床応用例－, 第 20 回日本耳科学会総会, 松山市, (2010)
西村忠己, 福田芙美, 斉藤　修, 宮前了輔, 岡安　唯, 下倉良太, 高木悠哉, 細井裕司, 軟骨伝導補聴器の開発(第２報）－呈示部位による感度差－, 第５５回日本聴覚医学会総会, 奈良市, (2010)
下倉良太, 高木悠哉, 西村忠己, 細井裕司, 軟骨伝導補聴器の開発(第 3 報）－外耳道内の音響特性－, 第５５回日本聴覚医学会総会, 奈良市, (2010)
岡安　唯, 西村忠己, 山下哲範, 中川誠司, 吉田悠加, 柳井修一, 長谷芳樹, 細井裕司, 骨

導超音波語音の母音刺激長に対するミスマッチフィールド, 第５５回日本聴覚医学会総会, 奈良市, (2010)
高木悠哉，下倉良太，柳井修一，西村忠己，細井裕司, 隣室から聞こえる透過騒音の研究～音の評価と不快感について～, 第５５回日本聴覚医学会総会, 奈良市, (2010)
吉田悠加，西村忠己，福田芙美，齋藤　修，細井裕司, 補聴器特性図から算出した利得とファンクショナルゲインの関係, 第５５回日本聴覚医学会総会, 奈良市, (2010)
齋藤　修，西村忠己，吉田悠加，福田芙美，柳井修一，細井裕司, 補聴器適合検査のための雑音不可時の語音明瞭度の検討, 第５５回日本聴覚医学会総会, 奈良市, (2010)
呉将延，猿渡洋，鹿野清宏，細井裕司, 両耳補聴器における ICA に基づく雑音推定を用いた平均二乗誤差最小化短時間振幅スペクトル推定法, 日本音響学会関西支部第 13 回若手研究者交流研究発表会, 京都市, (2010)
高木悠哉，下倉良太，柳井修一，細井裕司, 質問紙を用いた住宅内透過騒音の音評価に関する研究, 日本音響学会騒音・振動研究会, 京都市, (2010)

H．知的財産権の出願・登録状況

1. 特許取得

登録１件　特許番号：4541111

発明の名称：骨伝導振動子及び骨伝導受話装置

2. 実用新案登録

なし

3.その他

なし

II. 研究成果の刊行に関する一覧表

雑誌

発表者氏名	論文タイトル名	発表誌名	巻号	ページ	出版年
Takefumi Sakaguchi, Hiroshi Hosoi	Acoustical analysis of tympanoplasty with soft posterior meatal wall reconstruction	The Mediterranean Journal of Otology	Vol. 4, Supplement 1	137-138	2008
Tadashi Nishimura, Hiroshi Hosoi	Progressive hearing loss in intracochlear schwannoma	Eur. Arch. Otorhinolaryngol.	Vol. 265	489-492	2008
Yamashita A, Nishimura T, Nakagawa S, Sakaguchi T, Hosoi H.	Assessment of ability to discriminate frequency of bone-conducted ultrasound by mismatch fields	Neurosci Lett.	2008 Jun 20; 438(2)	260-262	2008
Yoshiki Nagatani, Katsunori Mizuno, Takashi Saeki, Mami Matsukawa, Takefumi Sakaguchi, Hiroshi Hosoi	Numerical and experimental study on the wave attenuation in bone – FDTD simulation of ultrasound propagation in cancellous bone	Ultrasonics	48	607–612	2008
長谷芳樹，橘亮輔，阪口剛史，細井裕司	親密度別単語了解度試験用音声データセット(FW03)単音節音声ラウドネス校正	日本音響学会誌	Vol. 64, No. 11	647-649	2008
阪口剛史，斉藤修，細井裕司	軟骨導音の方向感に関する基礎的検討	日本音響学会2008年秋季研究発表会講演論文集		447-448	2008
阪口剛史，細井裕司	軟骨導補聴の基礎的検討	第53回日本聴覚医学会学術講演会予稿集	Vol.51 No.5	375-376	2008
西村忠己	突発性難聴の診断と治療	奈医報	21(1)	17-22	2008
西村忠己，細井裕司	語音聴力検査	JOHNS	Vol. 24, No. 5	719-723	2008

西村忠己, 山下哲範, 細井裕司	老年性難聴	神経内科	68(5)	436-441	2008
西村忠己, 岡安唯, 細井裕司	補聴器の基本知識	medecina	Vol. 45, No. 7	1303-1306	2008
西村忠己, 細井裕司	補聴器の最新知見　補聴器外来の実態と将来のあるべき姿-大学病院の補聴器外来-	JOHNS	Vol. 24, No. 9	1333-1336	2008
西村忠己, 吉田悠加, 細井裕司	高齢者の補聴器装用希望者の聞こえに関する自己評価と家族評価	Audiology Japan	51	123-129	2008
Nagatani Yoshiki, Mizuno Katsunori, Saeki Takashi , Matsukawa Mami, Sakaguchi Takefumi, Hosoi Hiroshi	Propagation of fast and slow waves in cancellous bone: Comparative study of simulation and experiment	Acoust. Sci. & Tech.	30(4)	257-264	2009
Nishimura Tadashi, Nakagawa Seiji, Yamashita Akinori, Sakaguchi Takefumi, Hosoi Hiroshi	N1m amplitude growth function for bone-conducted ultrasound	Acta Otolaryngol Suppl	129	28-33	2009
Akinori Yamashita, Tadashi Nishimura, Yoshiki Nagatani, Tadao Okayasu, Toshizo Koizumi, Takefumi Sakaguchi, Hiroshi Hosoi	Comparison between bone-conducted ultrasound and audible sound in speech recognition	Acta Otolaryngol Suppl	129	34-39	2009

Toshizo Koizumi, Tadashi Nishimura, Takefumi Sakaguchi, Masanori Okamoto, Hiroshi Hosoi	Estimation of factors influencing the results of tinnitus retraining therapy	Acta Otolaryngol Suppl	129	40-45	2009
Akinori Yamashita, Tadashi Nishimura, Yoshiki Nagatani, Takefumi Sakagushi, Tadao Okayasu, Shuichi Yanai, Hiroshi Hosoi	The effect of visual information in speech signals by bone-conducted ultrasound	NeuroReport	21	119-122	2010
細井裕司	軟素材による外耳道再建型鼓室形成術－20年間の経験と本法における外耳道入口部拡大法－	頭頸部外科	19	25-31	2009
細井裕司	語音聴力検査－最近の動向－	Audiology Japan	52	563-570	2009
柳井修一 ・阪口剛史・細井裕司・鈴木直人	住宅内透過騒音の因子構造の検討	行動科学	48	115-122	2010
赤坂咲恵，西村忠己，岡安唯，細井裕司	難聴者における57-S語表の単音別正答率の検討	Audiology Japan	53	69-75	2010
Hosoi Hiroshi, Yanai Syuichi, Nishimura Tadashi, Sakaguchi Takefumi, Iwakura Takashi, Yoshino K	Development of cartilage conduction hearing aid	Archives of Materials Science and Engineering	42	104-110	2010

西村忠己	特集・高齢者の補聴ー実地診療に役立つ最新の知識ー　補聴器の適応ー聴覚障害者の来院から適応決定までー	ENTONI	115	7-11	2010
福田芙美，柳井修一，西村忠己，清水直樹，細井裕司	軟骨伝導によるラット聴性脳幹反応の測定	日本音響学会聴覚研究会資料	40	531-534	2010
西村忠己，細井裕司	特集　耳鼻咽喉科・頭頸部外科の検査マニュアルー方法・結果とその解釈　Ⅰ．聴覚検査　４．補聴器適合検査	耳喉頭頸	82	29-34	2010
細井裕司	特集・高齢者の補聴ー実地診療に役立つ最新の知識ー　補聴器フィッティングの全体像の理解	ENTONI	115	1-5	2010
呉将延，猿渡洋，鹿野清宏，細井裕司	ICAによる雑音推定に基づいた平均二乗誤差最小化短時間振幅スペクトル推定法の両耳補聴器への応用	日本音響学会講演論文集	2-9-8	691-694	2011
斉藤修，西村忠己，吉田悠加，福田芙美，柳井修一，細井裕司	補聴器適合検査のための雑音負荷時の語音明瞭度の検討	Audiology Japan	54	147-152	2011
吉田悠加，西村忠己，福田芙美，斉藤修，細井裕司	補聴器特性図から算出した利得とファンクショナルゲインの関係	Audiology Japan	54	118-122	2011
Tadashi Nishimura, Tadao Okayasu, Yuka Uratani, Fumi Fukuda, Osamu Saito, Hiroshi Hosoi	Peripheral perception mechanism of ultrasonic hearing	Hearing Research	In press	In press	2011

Tadao Okayasu, Tadashi Nishimura, Akinori Yamashita, Seiji Nakagawa, Yoshiki Nagatani, Shuichi Yanai, Yuka Uratani Yuka, Hiroshi Hosoi	Duration-dependent growth of N1m for speech-modulated bone-conducted ultrasound	Neuroscience Letters	In press	In press	2011

III. 研究成果の刊行物・別刷

Objectives: To investigate hearing 1 and 3 years after cholesteatoma surgery performed at the Otosurgical Section at the Department of Otolaryngology in Uppsala. 135 patients at all ages undergoing cholesteatoma surgery were investigated.

Surgical technique: All patients were operated with total or partial removal of the posterior bony canal wall with reconstruction of the bony wall, ear drum, ossicular chain and obliteration of the mastoid cavity.

Surgical outcome: 8 % of the patients underwent a columella revision surgery. In half of these a revision surgery was indicated due to recurrency, and in half due to residual cholesteatoma. All patients were audiologically evaluated pre- and postoperatively after 1 and 3 years. All patients were examined by the same surgeon.

Conclusion: Our results show that with the reconstruction technique used in connection with cholesteatoma surgery a good and long-lasting improvement in hearing may be obtained.

OP213 - Hearing Result of the Surgery for Cholesteatoma [216]

Okuno Taeko

Mitsui Memorial Hospital - Japan

Objective: Hearing result of the surgery for cholesteatoma was studied.

Material and methods: Two hundreds and thirty nine ears with middle ear cholesteatoma were operated in our hospital from July 1993 to October 2003.Hearing result of the surgery was studied according to the type of the cholesteatoma.

Results: There were 142 male and 97 female ears. The average age of the subjects was 41.1 years with a standard deviation of 19.7 years. The range was from 3 to 74 years.

Forty seven per cent of the cases had attic type cholesteatoma. Marginal type cholesteatoma was found in 17 %, central perforation with cholesteatoma in 8 %, and congenital cholesteatoma in 13 %. Average age at the time of ear surgery of attic cholesteatoma group was 43.2 years, average age of marginal group was 48.5 years, average age of central perforation with cholesteatoma group was 57.6 years and average age of congenital cholesteatoma group was 22.8 years. Tympanoplasty type I was carried out in 16%, type II in 3%, type III (including type III interposition and type III with columella) in 49%, and type IV (including type IV with columella) in 20%. Tympanoplasty for attic cholesteatoma ear resulted in a successful hearing rate of 76.8% Tympanoplasty for marginal cholesteatoma ear resulted in 63.2 % of successful rate and tympanoplasty for central perforation with cholesteatoma resulted in 70.0%.

OP214 - Ear Status after Cholesteatoma Surgery - Interim Results of a Long Term Prospective Study [132]

Noam Yehudai, Michal Luntz

Bnai Zion Medical Center, Haifa - Israel.

Objectives: To evaluate ear condition of children and adults undergoing cholesteatoma surgery in a referral otologic center.

Design: Demographic and clinical data was collected from 132 consecutive cholesteatoma surgeries. Ear status was established at the last patient's follow up visit to the out-patient clinic.

Results: 79 children (mean age 11.9 years) and 53 adults (mean age 40.3 years) were included. 39.4% of patients had a previous surgery before presenting to our department. Canal-wall up mastoidectomy with tympanoplasty was performed in 46% of the children and 30% of adults, canal wall down mastoidectomy with tympanoplasty (modified radical) was performed in 25% and 6% respectively, and canal wall down (radical) mastoidectomy was performed in 29% and 64% respectively. A planed second look was performed in 76.8% of children and 63.2% of adults. A revision of the radical cavity was done in 39.1% of children and 14.7% of adults. After a mean follow up period of 3.4 years (range 0.5-9.1), 9% of children and 7.5% of adults were lost to follow up. a dry ear was achieved in 78.5% of children and 73.6% of adults.

Conclusions: Pre-operatively all patients had a chronic discharging unsafe ear. Meticulous follow up is essential for achieving the goals of treatment but heavily depends on the cooperation of the patient, the family, the primary care physician and the medical insurance, which must fully internalized the absolute need for a life long dedicated follow up. The results show that it is possible to achieve a relatively comfortable ear in most patients, but unrealistic to assure dry ear for all cholesteatoma patients, even when cholesteatoma is eradicated. Suboptimal patient's compliance for periodic long term post-follow up visits was identified as a crucial obstacle for better results.

Keywords: cholesteatoma, post operative, follow up, compliance

OP215 - Acoustical Analysis of Tympanoplasty with Soft Posterior Meatal Wall Reconstruction [221]

Takefumi Sakaguchi

Nara Medical University - Japan

In the tympanoplasty, soft or hard materials are used in reconstructing posterior meatal wall. We have performed tympanoplasty with reconstruction of the soft posterior meatal wall for the prevention of post-operative retraction pocket formation for 18 years. Our method is characterized by the reconstruction of the soft posterior meatal wall, nonobliteration with permanent or temporary materials, including Gelfoam, no use of a Palva flap and the use of fibrin glue for attaching the fascia to the posterior meatal skin. None of the patients experienced post-operative narrow-neck retraction pocket formation, and whenever aeration of the middle ear was disturbed after the operation, a balloon-like retraction in various degrees which depends on each patient's aeration disturbance was observed.

Some suggests possibility of larger energy loss to bring about when the posterior meatal wall is reconstructed by soft materials compared to by hard ones. Hence, we calculated the transmitted acoustic power in the auditory pathway for both soft and hard posterior meatal walls in order to

elucidate the difference between these two in sound conduction effect.

We made three types of models which represented a hard wall, a soft wall without balloon-like retraction (i.e. normal position) and a soft wall with balloon-like retraction. We used a finite-difference time-domain method to calculate the acoustic power on both the ear drum and the columella for 500 Hz, 1 kHz and 2 kHz pure tone inputs. As a result, we did not find any obvious difference among these three conditions in efficiency of sound conduction.

OP216 - Evaluation of Prognostic Factors and Middle Ear Risk Index(MERI) in Tympanoplasty [334]

Ercan Pınar, [1]Kerim Sadullahoğlu, [1]Semih Öncel, Çağlar Çallı

İzmir Ataturk Training and Research Hospital ENT Clinic - Turkey

Objective: The aim of this study was to examine the effects of the prognostic factors and MERI on success rate of tympanoplasty.

Materials and Methods: The charts of 231 patients who underwent tympanoplasty operations between January 2002 and September 2007 were reviewed in this study. Patients were evaluated after 6 months postoperatively. Prognostic factors such as age, sex, presence of systemic diseases(diabetes mellitus and hypertension), site and size of perforation, duration of dry period, presence of hyaline plaque within tympanic membrane, operation type, status of the opposite ear, score of the MERI at presentation were investigated.

Results: The overall success rate was 74.4 %. Based on the univariate analysis, site and size of perforation, status of the opposite ear, absence of hyaline plaque within tympanic membrane, duration of dry period,operation type and low MERI score were found to be a statistically significant prognostic factors affecting success rate ($p<0.05$). Multivariate analysis was carried out on these significant prognostic factors and yielded the following results: healthy opposite ear(OR:5.64), size of perforation (OR:8.11), absence of hyalin plaque within tympanic membrane (OR:4.01), duration of dry period (OR:0.21) and low MERI score (OR:87.1).

Discussion: The goals of successful tympanoplasty are the removal of the pathology and achievement of a mucosal-lined middle ear cleft with an intact tympanic membrane. There are various prognostic factors reported in the literature influencing the success rate. Kartush introduced the MERI for tympanoplasty prognosis. The MERI combines the known preoperative and intraoperative risk factors. Multiple studies cited success rate from 60 to 90% in tympanoplasty, success rate was found 74.4% in this study.

Conclusion: Based on the results of this study, size of perforation, healthy opposite ear, absence of hyaline plaque within tympanic membrane, dry ear and low MERI were found to be a significant prognostic factors. Physician should be kept in mind these prognostic factors preoperatively to increase the success rate of tympanoplasty.

Keywords: tympanoplasty, prognostic factors.Middle Ear Risk Index (MERI)

OP217 - Long Term Functional Outcome of Canaloplasty in Congenital Atresia [665]

[1]Joost Van Dinther, [1]Thomas Somers, Erwin Offeciers

University Department of Otorhinolaryngology, Sint Augustinus Hospital, Wilrijk, Antwerp - Belgium

Objective: To evaluate the long term functional outcome of canaloplasty in congenital (partial) atresia of the outer ear canal. In atresia cases it is necessary to carefully weigh the pro's and cons of reconstructive surgery, because bone anchored hearing aids and active middle ear implants offer a possible alternative and because of the well documented short and long term morbidity of reconstructive surgery.

Materials and methods: Our database of 116 patients (148 ears) with congenital canal atresia was retrospectively evaluated. The long term functional outcome of canaloplasty was evaluated, in two classes of stenotic ear canals: the completely stenotic (atretic) canals versus the partially (filiform) canals.

Results: A total of 33 ears with completely (atretic) or partially stenotic (filiform) outer ear canals were treated by canaloplasty for functional purposes. The long term result (mean follow up of 8 years) showed an improvement of the PTA with 16 dB for the whole group ($n=33$), of 10 dB for the atretic group ($n=24$) and 33 dB for the filiform group ($n=9$).

Discussion: In our experience reconstruction of completely atretic ear canals only yields short term satisfactory results. The absence of migratory behaviour of the skingrafts, transplanted to cover the medial part of the new canal, prevents a normal self cleaning of the canal. This causes chronic myringitis resulting in scar tissue formation and partial restenosis of the canal.

The initially present functional gain deteriorates. In contrast, if a filiform canal is present, these skin remnants are carefully preserved to cover part of the new canal. Those ears keep their normal self cleaning mechanism in the long term. As a consequence these ears remain anatomically and functionally stable.

Conclusion: Therefore we only apply reconstructive surgery in cases with a filiform ear canal. All completely stenotic cases are only offered the option of a bone anchored hearing aid.

Keywords: atresia, agenesia, functional surgery, canaloplasty, long term results, BAHA

OP218 - Analysis of the Properties and Treatment Outcomes of Acquired Cholesteatoma in Children Compared with Adults [640]

[1]John Hamilton, [1]Niranjan Raghava

[1]Gloucestershire Hospitals Trust - UK

It is recognised that cholesteatoma behaves differently in children compared to adults.

Objectives: The aim of this study is to quantitatively analyses the characteristics of pediatric cholesteatoma and compare its behaviour with that of adults. A further aim of this study is to compare the response to intact canal cholesteatoma surgery of pediatric and adult ears.

Eur Arch Otorhinolaryngol (2008) 265:489–492
DOI 10.1007/s00405-007-0483-x

CASE REPORT

Progressive hearing loss in intracochlear schwannoma

Tadashi Nishimura · Hiroshi Hosoi

Received: 6 September 2007 / Accepted: 24 September 2007 / Published online: 12 October 2007

Abstract Intralabyrinthine schwannomas are rare tumors. It is difficult to diagnose them, and their hearing disturbance has not been sufficiently elucidated. Recently, however, the development of the imaging technology enables the diagnosis of intracochlear schwannoma before operation. We experienced a case of intracochlear schwannoma diagnosed with mild hearing loss. Pure tone audiometry (PTA) showed hearing loss at mid-frequency, with a mean threshold of 33.3 dB. Magnetic resonance imaging (MRI) revealed an abnormal lesion in the cochlea. Finally, PTA showed profound deafness and MRI revealed invasion of the schwannoma into the fundus of the internal auditory canal. Considering the progress and the results of audiometric examinations, hearing disturbance by intracochlear schwannoma is investigated in this report.

Keywords Intracochlear schwannoma · Magnetic resonance imaging · Auditory brainstem response

Introduction

Acoustic neuromas usually arise from the vestibular nerve within the internal auditory canal (IAC) and cerebellopontine angle. Intralabyrinthine schwannomas are uncommon and difficult to diagnose. They are usually diagnosed accidentally during labyrinthectomy for Meniere's disease [1, 2], vestibular neurotomy [3], cochlear implantation [4], or autopsy [5]. Therefore, hearing disturbance by intralabyrinthine schwannomas has not been sufficiently elucidated. We present a case of intracochlear schwannoma diagnosed with mild hearing loss. In this case, hearing loss had progressed to profound deafness over approximately 2 years.

T. Nishimura (✉) · H. Hosoi
Department of Otorhinolaryngology,
Nara Medical University, 840 Shijo-cho,
Kashihara, Nara 634-8521, Japan
e-mail: t-nishim@naramed-u.ac.jp

Case report

A 48-year-old woman with idiopathic thrombocytopenic purpura (ITP) noticed the sudden onset of right hearing loss and tinnitus. Ten days after the onset, she visited a hospital to have her hearing assessed. Pure tone audiometry (PTA) showed a notch at 500 Hz in the right ear (Fig. 1). She received a 2-week short tapered course of high-dose steroid therapy from the hospital. One week after the therapy, her hearing loss became worse, and she was referred to our department.

When she first visited our department, she presented with hearing loss, tinnitus and fullness of the right ear. No vestibular or neural symptoms were present. Otoscopic examination of the ear revealed normal tympanic membranes. Pure tone audiometry showed hearing loss at mid-frequency, with a mean threshold of 33.3 dB (the average of 500, 1,000 and 2,000 Hz) (Fig. 1). Speech discrimination scores in the right and left ears were 90% at 50 dB and 100% at 40 dB, respectively. Although fixed-frequency Bekesy audiometry showed Type I, alternate binaural loudness balance (ABLB) test revealed complete recruitment (Fig. 2). Transient evoked otoacoustic emission (TEOAE) levels in the right and left ears were 6.4 (reproducibility was 69%) and 8.2 dB (reproducibility was 77%), respectively. Distortion product otoacoustic emission (DPOAE) levels at 1 kHz were in the region of uncertainty in the right ear (Fig. 3). Auditory brainstem response (ABR) threshold

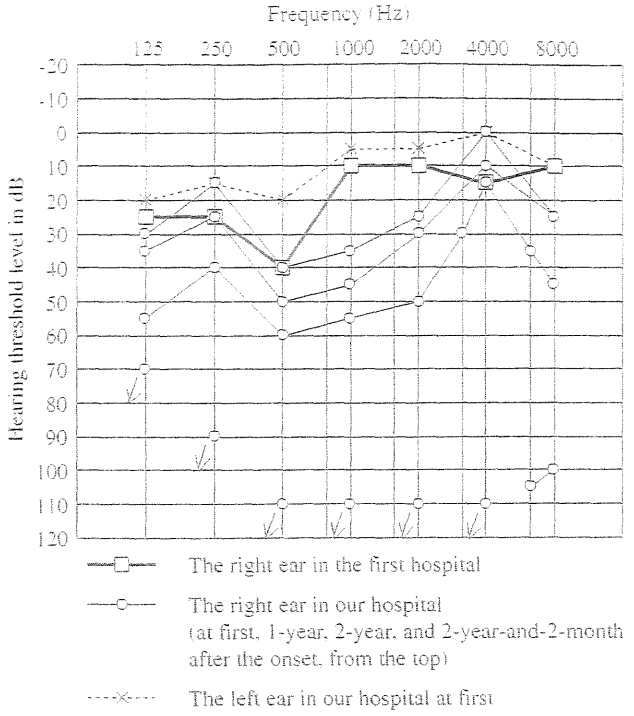

Fig. 1 Changes in pure tone audiometry for approximately 2 years before profound deafness. The *arrows* at the bottom of audiogram mean no response

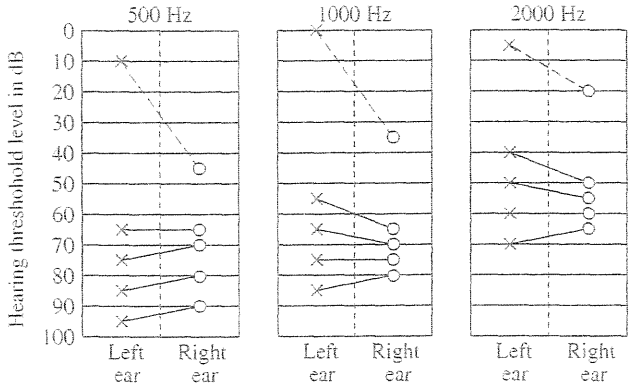

Fig. 2 Plot of loudness balance results by laddergram

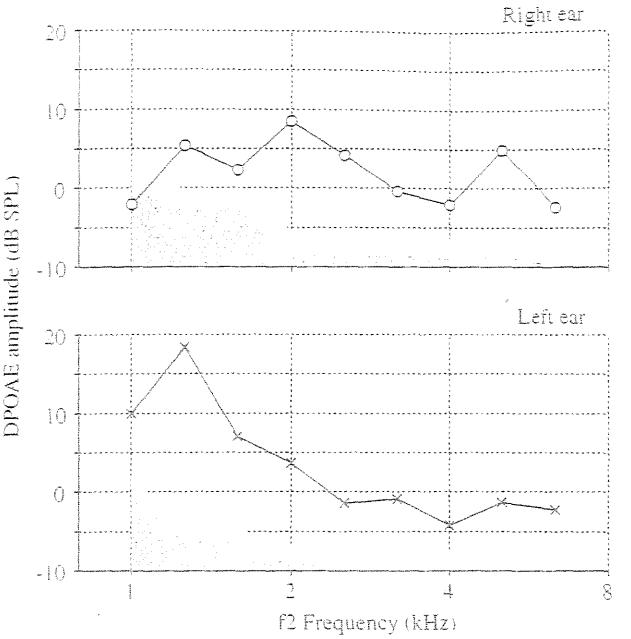

Fig. 3 Mean amplitude of distortion product otoacoustic emissions and noise floor at each *f2* frequency. The *colored* areas near the bottom indicate the average background noise floor levels

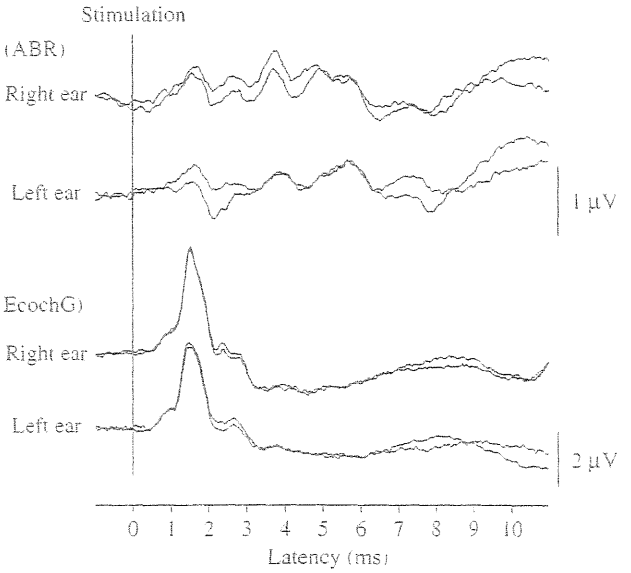

Fig. 4 Auditory brainstem response and electrocochleogram (EcochG) evoked by clicks at the intensity of 80 dB nHL

in the right ear was 20 dB nHL, equal to the left. No increases in absolute peak latency (waves I, III and V) and interpeak latency (I–III, III–V and I–V) were obtained (Fig. 4). Electrocochleogram showed normal waveforms (Fig. 4). Laboratory studies were normal except for a low platelet count due to ITP. Although another short tapered course of high-dose steroid and additional prostaglandin E1 therapy were performed, her hearing did not improve.

Three months after onset, magnetic resonance imaging (MRI) was performed. Although no abnormal lesion was obtained on T1- and T2-weighted images, gadolinium-enhanced MRI showed a small enhancing lesion in the cochlea (Fig. 5). Constructive interference in the steady-state (CISS) sequence, which can provide high-resolution images with good contrast between cerebrospinal fluid and solid structures, revealed the absence of a fluid signal in the middle turn of the cochlea, while no abnormal fluid signal was evident in IAC (Fig. 6). The lesion was interpreted as being either a small schwannoma or inflammation. Since the same enhancement was obtained on the second MRI

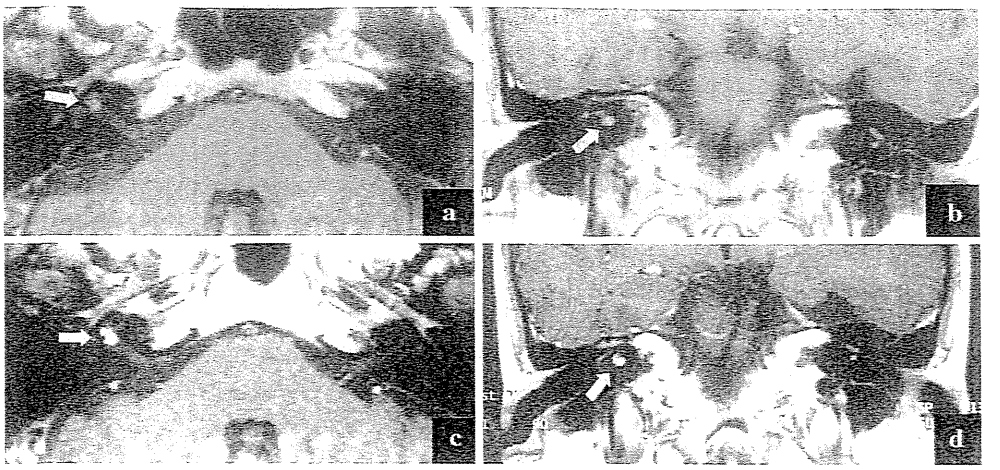

Fig. 5 Magnetic resonance imaging with gadolinium contrast showing axial (a, c) and coronal views (b, d). Upper (a, b) and lower (c, d) images were obtained at 2 months and 2 years and 2 months after onset, respectively. *Arrows* indicate enhancing lesions

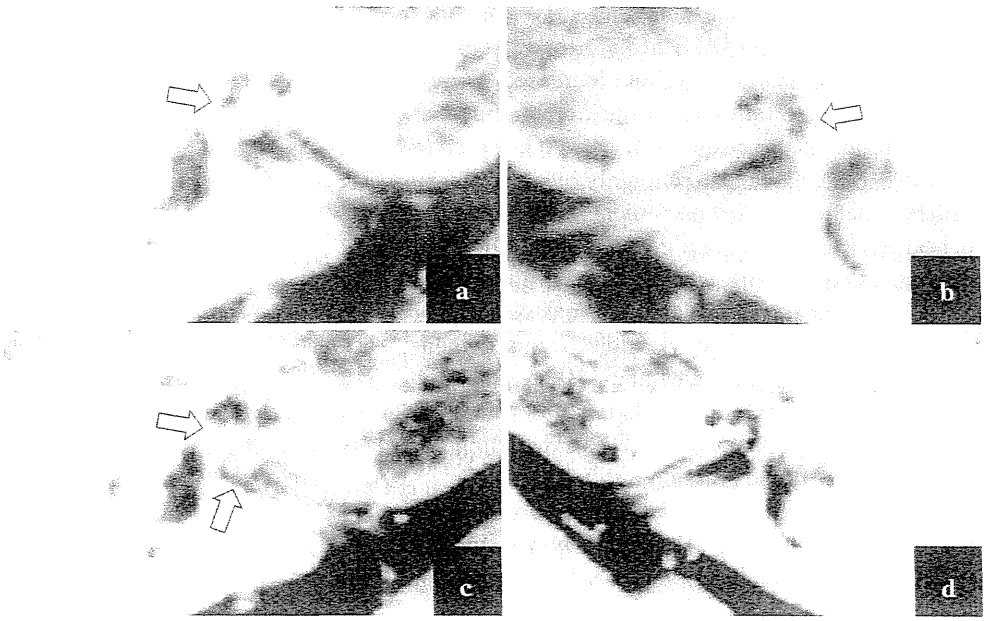

Fig. 6 Constructive interference in steady-state sequence obtained at 2 months (a, b) and 2 years and 2 months (c, d) after onset. In image a, the *arrow* indicates the absence of fluid signal in the middle turn of the cochlea that is not obtained on the normal side (b). In image c, the absence of fluid signal is clearly evident not only in the cochlea but also in the fundus of the internal auditory canal

performed 3 months later, we diagnosed this case as intracochlear schwannoma.

During the 2 year follow-up, the threshold in the right increased gradually (Fig. 1). Two years after the first episode, she reported progressive loss of hearing and a third MRI was performed 2 months later. In gadolinium-enhanced MRI, two enhancing lesions were distinguishable, one in the cochlea and the other in the fundus of the IAC (Fig. 5). Furthermore, the absence of a fluid signal on the CISS sequence spread in the middle turn of the cochlea and in the fundus of the IAC (Fig. 6). At the time, PTA showed profound hearing loss in the right ear. TEOAE and DPOAE were absent. Auditory brainstem response was not recorded at 100 dB nHL. She received high-dose steroid therapy, resulting in no improvement in her hearing. Considering the lack of vertigo episodes and the risk of operation due to ITP, she chose follow-up with serial MRI.

Discussion

In cases of schwannoma in IAC, audiometric examinations generally show no cochlear disorders but retrocochlear disorders; however, in our case, retrocochlear disorders were not evident on audiometric examination. Recruitment was obtained in the ABLB test and low response in DPOAE was obtained in the range which was almost consistent with hearing loss in PTA; therefore, hearing disturbance in our case was considered as a cochlear disorder, probably involved by occupation of the cochlea by schwannoma. Our case suggests that the presence of cochlear disorders in audiometric examinations, such as recruitment, does not rule out the possibility of intracochlear schwannoma.

One of the most important audiometric examinations for the diagnosis of schwannoma is the ABR test. For schwannoma in IAC, the ABR test usually shows an abnormal response associated with retrocochlear disorders;

however, there have been only a few reports about ABR in intracochlear schwannoma. Gersdorff et al. [6] reported an increase in the absolute latency of the first peak in ABR. In their case, PTA showed a mean threshold of 85 dB for frequencies between 250 and 2,000 Hz. The curve was ascendant for the higher frequency, and the threshold at 8 kHz was 30 dB; however, schwannoma was pointed out in the basal turn of the cochlea and in the fundus of IAC. Therefore, the cochlear partitions occupied by schwannoma in the cochlea were different from those related to hearing loss in the audiogram. Thus, hearing loss in their case may be the retrocochlear type rather than cochlear. On the other hand, in our case, ABR was normal at the beginning of follow-up. Considering the relationship between hearing loss in the audiogram and the occupation of schwannnoma in the cochlea, hearing loss was first interpreted as a cochlear disorder. During follow-up before profound deafness, the hearing threshold increased gradually and equally at all frequencies. Considering that the schwannoma had invaded the fundus of the IAC, the progress of hearing loss may be caused mainly by retrocochlear disorders due to invasion. When PTA showed profound hearing loss in the right ear, TEOAE, DPOAE and ABR were absent. This is probably because both cochlear and retrocochlear lesions caused too severe deafness for any recordings to be possible. Thus, when schwannoma localizes in the cochlea, the ABR test probably does not show retrocochlear disorders. Observation of the retrocochlear type in the ABR test is the finding to indicate the possibility of the invasion into IAC.

Intracochlear schwannoma may be difficult to diagnose even with gadolinium-enhanced MRI [7]. However, in our case, a gadolinium-enhancing lesion was detected in the cochlea, and we suspected intracochlear schwannoma. While Donnelly et al. [8] indicated the usefulness of the CISS sequence in defining intracochlear lesions, the CISS image in our case was also of great benefit to the evaluation of intracochlear schwannoma. Thus, the development of the imaging technology help the diagnosis of intracochlear schwannoma. As our case, intracochlear schwannoma will be diagnosed at the early stage with mild hearing loss in the future, if appropriate examination and evaluation are performed. In order not to overlook it, it is necessary to pay attention to abnormal lesions within the cochlea or vestibule, and a suspicious lesion should be confirmed by a repeat scan.

References

1. Vernick DM, Graham MD, McClatchey KD (1984) Intralabyrinthine schwannoma. Laryngoscope 94:1241–1243
2. Huang TS (1986) Primary intralabyrinthine schwannoma. Ann Otol Rhinol Laryngol 95:190–192
3. Sataloff RT, Roberts BR, Feldman M (1988) Intralabyrinthine schwannoma. Am J Otol 9:323–326
4. Kronenberg J, Horowitz Z, Hildesheimer M (1999) Intracochlear schwannoma and cochlear implantation. Ann Otol Rhinol Laryngol 108:659–660
5. Ohtani I, Suzuki C, Aikawa T (1990) Temporal bone pathology in intracochlear schwannoma with profound hearing loss. Auris Nasus Larynx 17:17–22
6. Gersdorff MC, Decat M, Duprez T, Deggouj N (1996) Intracochlear schwannoma. Eur Arch Otorhinolaryngol 253:374–376
7. Green JD Jr, McKenzie JD (1999) Diagnosis and management of intralabyrinthine schwannomas. Laryngoscope 109:1626–1631
8. Donnelly MJ, Daly CA, Briggs RJ (1994) MR imaging features of an intracochlear acoustic schwannoma. J Laryngol Otol 108:1111–1114

Neuroscience Letters 438 (2008) 260–262

Contents lists available at ScienceDirect

Neuroscience Letters

journal homepage: www.elsevier.com/locate/neulet

Assessment of ability to discriminate frequency of bone-conducted ultrasound by mismatch fields

Akinori Yamashita[a,*], Tadashi Nishimura[a], Seiji Nakagawa[b], Takefumi Sakaguchi[a], Hiroshi Hosoi[a]

[a] Department of Otolaryngology, Nara Medical University, 840 Shijo-cho, Kashihara, Nara 634-8522, Japan

[b] Institute for Human Science and Biomedical Engineering, National Institute of Advance Industrial Science and Technology (AIST), 1-8-31 Midorigaoka, Ikeda, Osaka 563-8577, Japan

ARTICLE INFO

Article history:
Received 25 June 2007
Received in revised form 21 December 2007
Accepted 30 March 2008

Keywords:
Ultrasound
Magnetoencephalography
Bone conduction
Mismatch fields
Frequency modulation

ABSTRACT

According to previous studies, ultrasound can be perceived through bone conduction and ultrasound amplitude modulated by different speech sounds can be discriminated by some profoundly deaf subjects as well as the normal-hearing. These findings suggest the usefulness of development of a bone-conducted ultrasonic hearing aid (BCUHA) for profoundly deaf subjects. In this study, with a view to developing a frequency modulation system in a BCUHA, the capability to discriminate the frequency of sinusoidal bone-conducted ultrasound (BCU) was evaluated by measuring mismatch fields (MMF). We compared MMFs between BCU (standard stimuli were 30 kHz, and deviant stimuli were 27 and 33 kHz) and air-conducted audible sound (ACAS; standard stimuli were 1 kHz, and deviant stimuli were 900 and 1100 Hz). MMFs were observed in all subjects for ACAS, however, not observed in a few subjects for BCU. Further, the mean peak amplitudes of MMF for BCU were significantly less than those for ACAS. These findings indicate that the discrimination capability of frequency of sinusoidal BCU is inferior to that of ACAS. It was also demonstrated that normal hearing could to some extent discriminate differences in frequency in sinusoidal BCU. The results indicate a possibility of transmission system for language information making use of frequency discrimination.

Generally speaking, human listeners perceive sound signals through air conduction from 20 to 20,000 Hz. Sound with frequency over 20 kHz is termed "ultrasound". Until half a century ago, it was thought that ultrasound could not be perceived. However, Gavreau reported in 1948 that ultrasound was audible when delivered by bone conduction [5]. Several researchers subsequently reported interesting perceptual characteristics of bone-conducted ultrasound (BCU), which differ markedly from those of audible sound. For instance, the subjective pitch of BCU is independent of its frequency [2,3] and it is perceived as if it were from air-conducted stimuli of 8–16 kHz [2,3,10]. In addition, BCU can mask perception of air-conducted audible sound (ACAS) of 10–14 kHz and this masking of ACAS is independent of ultrasonic frequency. The dynamic range of BCU is narrower than that of ACAS [9]. Interestingly, some profoundly deaf patients can hear BCU. Lenhardt et al. reported that BCU hearing supported frequency discrimination and speech detection in some deaf patients as well as normal-hearing subjects by [7]. Furthermore, Hosoi et al. found using magnetoencephalography that BCU stimuli activate the auditory cortex, and that ultrasound amplitude modulated by different speech sounds can be discriminated in the auditory cortex in some profoundly deaf subjects [6]. These findings suggest the possibility of development of a bone-conducted ultrasonic hearing aid (BCUHA), which could be used by elderly hearing-impaired and profoundly deaf subjects [8].

For development of such a hearing aid, it is necessary to determine the most effective method of transmission of language information. Corso founded that BCU perception is characterized by poor frequency discrimination, although auditory perception in ACAS is characterized by excellent frequency discrimination [1]. This has been concluded from the finding that subjective pitch elicited by BCU stimulation is independent of its frequency and similar to that for the highest ACAS. Lenhardt, using a psychoacoustical method, reported that just noticeable pitch differences in the ultrasonic range were on the order of 10% of the stimulus frequency, although that in the auditory range were between 0.4 and 1.0% [7]. These studies have found that ability to discriminate the frequency of BCU is inferior to that of ACAS. However, no study has

* Corresponding author. Tel.: +81 744 29 8887; fax: +81 744 24 6844.
E-mail address: akinori@naramed-u.ac.jp (A. Yamashita).

0304-3940/$ – see front matter © 2008 Elsevier Ireland Ltd. All rights reserved.
doi:10.1016/j.neulet.2008.03.086

evaluated ability to discriminate the frequency of sinusoidal BCU objectively. In this study, to assess a possibility of development of a frequency modulation system in a BCUHA, we measured discrimination capability of the frequency of sinusoidal BCU by magnetoencephalography.

Twelve right-handed volunteers (aged 20–30 years, 4 females and 8 males) with normal hearing and no history of neurological diseases took part in the study. They gave written informed consent after being informed of the nature and purpose of this study.

To evaluate capability to discriminate BCU, comparison was made with capability to discriminate ACAS since previous studies more frequently used ACAS than BCU. We measured mismatch fields (MMFs) for BCU and ACAS, in cases in which the frequency deviated 10% from standard frequency. BCU and ACAS were presented in separate sequences. Each sequence consisted of a standard stimulus (probability 90%) and two types of deviant stimuli (probability 5% each), with all stimuli delivered in random order to the subject. More than 100 responses evoked by deviant stimuli were averaged. After averaging of MMFs, one of the deviant stimuli was continually and successively delivered more than 100 times as a comparison stimulus. The other deviant stimulus was then delivered in the same fashion. In a sequence of BCU, we used 30 kHz BCU as a standard stimulus and 27 and 33 kHz BCU as deviants and comparison stimuli. On the other hand, in ACAS sequences, we used 1000 Hz ACAS as a standard stimulus and 900 and 1100 Hz ACAS as deviant and comparison stimuli. The intensities of BCU and ACAS were set at 15 and 60 dB SL, respectively. The duration was set at 50 ms, including 5 ms rise/fall times, and the interstimulus interval was varied randomely between 0.9 and 1.1 ms. During the experiment, the subject was watching a self-chosen movie without sound and was instructed to pay no attention to the auditory stimuli.

Recording of the brain activation evoked by BCU and ACAS was performed in a magnetically shielded room using a 122-channel whole-head neuromagnetometer (Neuromag-122; Neuromag Ltd., Helsinki, Finland). All the sounds were generated by a function generator (WF1946; NF Electronic Instruments Co., Yokohama, Japan). The ultrasound signal was increased through a high-speed power amplifier (HSA4011; NF Electronic Instruments Co, Yokohama, Japan). Sound intensity was controlled by a programmable attenuator in the dB scale (PA4; Tucker–Davis Technologies, Gainesville, FL). Ultrasound was delivered with a custom-made ceramic vibrator for MEG fixed on the left mastoid. The ACAS was emitted using an earphone (E-A-R TONE3A, Cabot Safety Co., Indianapolis, IN), and was delivered to the left ear through a plastic tube. MEG signals were measured, having been digitized at 400 Hz, and were band-pass-filtered through 0.03–100 Hz. Any responses including greater than 3000 fT/cm changes were rejected from further analysis. Averaged data were band-pass-filtered through 0.1–30 Hz off-line. The duration of analysis was 0.7 s, beginning 0.2 s prior to stimulus onset. The average during the 0.2 s prestimulus period served as the baseline. The neuromagnetometer used in this experiment has two pick-up coils in each position, which measure tangential derivatives, $\delta Bz/\delta x$ and $\delta Bz/\delta y$, of field component Bz. We determined:

$$B' = \sqrt{\left(\frac{\delta Bz}{\delta x}\right)^2 + \left(\frac{\delta Bz}{\delta y}\right)^2},$$

as the amplitude of the response. For determination of the MMF amplitude of each subject, we employed the maximum $B'z$ placed over the right temporal area.

The MMF was delineated by subtracting the comparison-stimulus responses from the deviant-stimulus response separately for each sequence and deviant type. We defined MMF as follows: peak latency ranged from 100 to 300 ms, peak amplitude was greater than 10 fT/cm, and the estimated equivalent current dipole was over the right temporal area and turned downward. We employed a channel where the largest MMF peak amplitude was observed with all stimuli. With this channel, each MMF peak amplitude and latency were measured. Amplitudes were normalized to the respective values obtained at the largest MMF peak amplitude in each subject. Differences in peak amplitude and peak latency between BCU and ACAS responses were tested for significance by two-ways ANOVA.

Clear N1m responses were observed in all subjects for all type of stimuli. N1m responses for all stimuli showed the maximum amplitude during 80 to 116 ms. Fig. 1 shows the response waveforms in a subject for 33 kHz BCU and 1100 Hz ACAS. In this subject, clear N1m and MMF responses were observed for all stimuli.

All subjects replied to detect the pitch change with change in frequency of ACAS and BCU. Although MMFs were observed in all subjects for ACAS, not observed in 3 subjects for 27-kHz and 1 subject for 33-kHz BCUs. The delineated MMF was elicited at

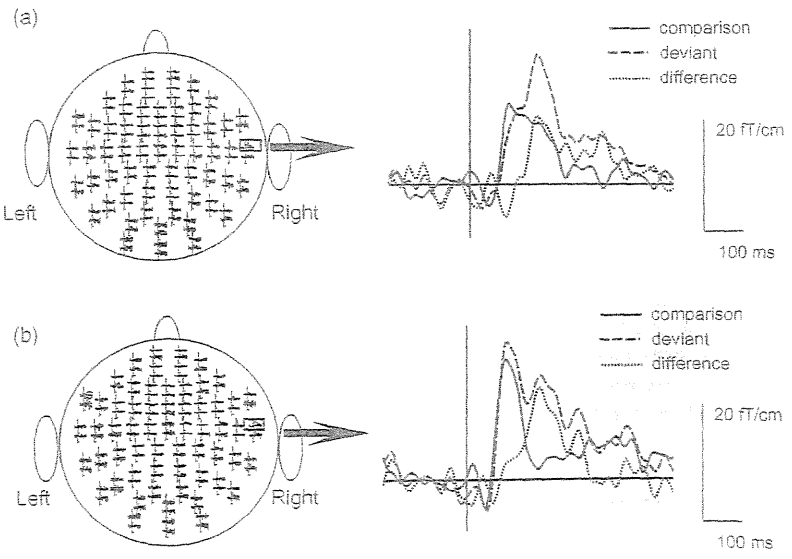

Fig. 1. Wave forms in a subject evoked by (a) 33-kHz BCU and (b) 1100-Hz ACAS. The sensor locations are shown in the left part, and the waveforms in the largest responses measured in the MEG channels in the right temporal region are enlarged in the right part.

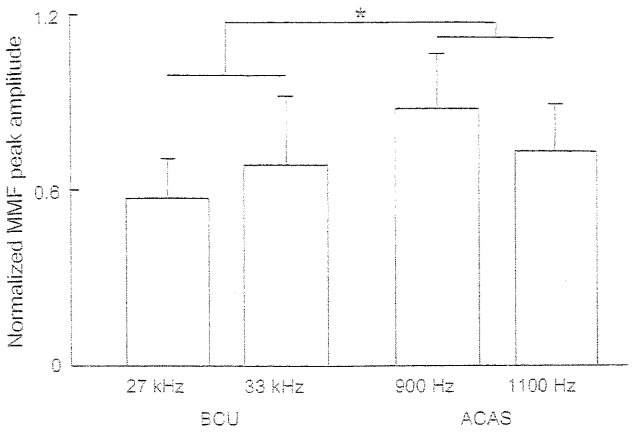

Fig. 2. Mean MMF peak amplitudes for BCU and ACAS. Vertical bars indicate standard deviations.

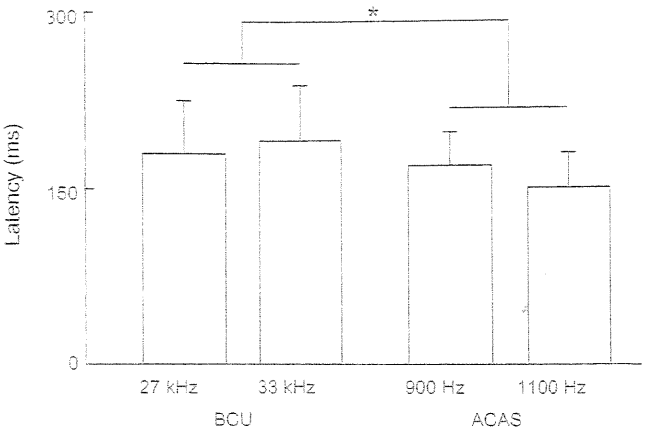

Fig. 3. Mean MMF peak latencies for BCU and ACAS. Vertical bars indicate standard deviations.

latencies of 180–200 ms for all frequencies. Fig. 2 shows normalized MMF peak amplitude. The mean peak amplitudes for BCU (27 and 33 kHz) were significantly less than those for ACAS (900 and 1100 Hz) ($p < 0.05$). Fig. 3 shows the mean peak latencies of MMF. The mean peak latencies for BCU were significantly later than those for ACAS ($p < 0.05$).

Although MMFs were observed in all subjects for ACAS, however, in only 9 and 11 subjects for 27- and 33-kHz BCUs, respectively. Even in case MMF were observed for BCU, MMF peak amplitude in BCU reached about three-fourths of that for ACAS. The peak amplitudes for BCU were significantly less than those for ACAS. Thus, capability to discriminate the frequency of BCU was inferior to that of ACAS, in agreement with previous reports.

Although most subjects detected pitch change with change in frequency of BCU, the amount of pitch change exhibited marked variation among our subjects. Previous studies reported similar findings; the subjective pitch elicited by ultrasonic stimulation was independent of its frequency, and it is perceived as if it were from air-conducted stimuli of 8–16 kHz. These characteristics of ultrasonic perception indicate that the pitch of BCU fluctuates and that pitch change is unstable. That is, the amount of pitch change exhibits large individual variation with a given change in stimulus frequency. In the range of ultrasonic frequency, increase in frequency does not always lead to subjective increase in pitch. These characteristic changes in pitch in the ultrasonic range may have been responsible for the variation in MMF we observed.

If BCU is to be used as a means of communication, language information must be modulated to within the ultrasonic range using amplitude modulation, frequency modulation, or so. For development of ultrasonic hearing aids, it will be necessary to determine which type of modulation is more effective. Fujimoto et al. reported good capability of frequency discrimination of BCU by amplitude modulation. The difference limens for frequency for pure tones modulated onto ultrasonic carriers was as small as that for air-conducted pure tones at 0.25–4 kHz [4]. On the other hand, no previous study has investigated ability to discriminate BCU using frequency modulation. The present study evaluated capability to discriminate frequency in sinusoidal BCU objectively using MEG. Our results objectively demonstrated that capability to discriminate the frequency of BCU was inferior to that of ACAS. However, it was also demonstrated that normal hearing could to some extent discriminate differences in frequency in sinusoidal BCU. In addition, it may be possible to improve frequency discrimination capability by training or improvement of sound processing. Therefore, further investigation is needed to determine the most appropriate transmission system for language information using ultrasound.

The present findings provide important clues to the development of the BCUHA. However, the characteristics of BCU hearing and the mechanisms of perception of BCU are still unclear. Further study is needed for development of the BCUHA in elderly hearing-impaired and profoundly deaf subjects.

References

[1] J.F. Corso, Bone-conduction thresholds for sonic and ultrasonic frequencies, J. Acoust. Soc. Am. 35 (1963) 1738–1743.
[2] B.H. Deatherage, L.A. Jeffress, H.C. Blodgett, A note on the audibility of intense ultrasonic sound, J. Acoust. Soc. Am. 26 (1954) 582.
[3] H.G. Dieroff, H. Ertel, Some thoughts on the perception of ultrasound by name, Arch. Otorhinolaryng 209 (1975) 277–290.
[4] K. Fujimoto, S. Nakagawa, M. Tonoike, Nonlinear explanation for bone-conducted ultrasonic hearing, Hear. Res. 204 (2005) 210–215.
[5] V. Gavreau, Audibillite de sons frequence elevee, C. R. 226 (1948) 2053–2054.
[6] H. Hosoi, S. Imaizumi, T. Sakaguchi, M. Tonoike, K. Murata, Activation of the auditory cortex by ultrasound, Lancet 351 (1998) 496–497.
[7] M.L. Lenhardt, R. Skellett, P. Wang, A.M. Clarke, Human ultrasonic speech perception, Science 253 (1991) 82–85.
[8] S. Nakagawa, Y. Okamoto, Y. Fujisaka, Development of a Bone-conducted Ultrasonic Hearing Aid for the Profoundly Sensorineural Deaf, Trans. Jpn. Soc. Med. Biol. Eng. 44 (1) (2006) 184–189.
[9] T. Nishimura, S. Nakagawa, T. Sakaguchi, H. Hosoi, Ultrasonic masker clarifies ultrasonic perception in man, Hear. Res. 175 (2003) 171–177.
[10] R. Pumphrey, Upper limit of frequency for human hearing, Nature 166 (1950) 571.

Ultrasonics 48 (2008) 607–612

Contents lists available at ScienceDirect

Ultrasonics

journal homepage: www.elsevier.com/locate/ultras

Numerical and experimental study on the wave attenuation in bone – FDTD simulation of ultrasound propagation in cancellous bone

Yoshiki Nagatani [a,*], Katsunori Mizuno [b,1], Takashi Saeki [b,1], Mami Matsukawa [b,1], Takefumi Sakaguchi [a,2], Hiroshi Hosoi [a,2]

[a] Department of Otorhinolaryngology, Nara Medical University, 840 Shijo-cho, Kashihara, Nara 634-8522, Japan
[b] Graduate School of Engineering, Doshisha University, 1-3 Miyakodani, Tatara, Kyotanabe, Kyoto 610-0321, Japan

ARTICLE INFO

Article history:
Received 20 August 2007
Received in revised form 23 April 2008
Accepted 23 April 2008
Available online 13 May 2008

Keywords:
Cancellous bone
Fast wave
X-ray CT
Three-dimensional elastic FDTD method

ABSTRACT

In cancellous bone, longitudinal waves often separate into fast and slow waves depending on the alignment of bone trabeculae in the propagation path. This interesting phenomenon becomes an effective tool for the diagnosis of osteoporosis because wave propagation behavior depends on the bone structure. Since the fast wave mainly propagates in trabeculae, this wave is considered to reflect the structure of trabeculae. For a new diagnosis method using the information of this fast wave, therefore, it is necessary to understand the generation mechanism and propagation behavior precisely. In this study, the generation process of fast wave was examined by numerical simulations using elastic finite-difference time-domain (FDTD) method and experimental measurements. As simulation models, three-dimensional X-ray computer tomography (CT) data of actual bone samples were used. Simulation and experimental results showed that the attenuation of fast wave was always higher in the early state of propagation, and they gradually decreased as the wave propagated in bone. This phenomenon is supposed to come from the complicated propagating paths of fast waves in cancellous bone.

1. Introduction

More reliable and less onerous diagnosis of osteoporosis is now expected in this aging society. Ultrasonic diagnosis system is considered as a strong tool, because ultrasonic wave reflects the elasticity. The current *in vivo* ultrasonic diagnosis technique called speed of sound/broadband ultrasound attenuation (SOS/BUA) method [1] is a simple indicator to describe bone properties. The SOS/BUA method gives the averaged ultrasonic wave speed and attenuation in a whole area including soft tissue, cortical bone, and cancellous bone, which seems difficult to show the complicated bone structure and the amount of mineral materials of each part. Therefore, a new index that can reflect detailed structure of bone is now required: e.g. Padilla et al. and Jenson et al. proposed a new indicator using backscattered wave from bone sample [2–4].

In order to improve the accuracy of ultrasonic diagnosis systems, our group has proposed a new evaluation idea, making use of the separation of longitudinal waves that pass through the cancellous bone [5–7]. We have reported the separation of longitudinal waves into fast and slow waves, especially depending on the alignment of bone trabeculae in cancellous bone. This interesting phenomenon is considered to become a strong tool for the diagnosis of osteoporosis because the wave propagation behavior apparently depends on the bone structure. However, the details of wave propagation in cancellous bone are not fully understood, because of the structural complexity and inhomogeneity of the bone.

In order to understand the wave propagation phenomena in the cancellous bone, there were some theoretical approaches. By Biot's theory [8,9] or stratified model [10], with the help of several parameters to describe the bone structure, we can predict the generation of fast and slow waves in cancellous bone. However, the selection of parameters such as porosity, bulk and shear moduli of solid part, fluid viscosity and permeability in Biot's theory seems to be very difficult.

One recent approach to understand the wave propagation is the direct analysis of wave equation. If the 3-D numerical simulation of wave propagation is successfully performed, it shall give us the visual image of complicated wave propagation in the bone. Luo et al. have reported the simulation results of wave propagation in cancellous bone using microCT model [11]. They investigated the wave speed and the attenuation values, however, they did not discuss the wave separation into fast and slow waves. Hosokawa has first reported the wave separation by a numerical solution of Biot's theory with finite-difference method [12]. Using a 3-D synchrotron

* Corresponding author. Tel.: +81 744 22 3051; fax: +81 744 24 6844.
E-mail addresses: naramed-u@nagatani.ne.jp (Y. Nagatani), mmatsuka@mail.doshisha.ac.jp (M. Matsukawa).
[1] Tel.: +81 774 65 6292; fax: +81 774 65 6801.
[2] Tel.: +81 744 22 3051; fax: +81 744 24 6844.

0041-624X/$ - see front matter © 2008 Elsevier B.V. All rights reserved.
doi:10.1016/j.ultras.2008.04.011

micro tomography of actual trabeculae, Bossy et al. [13] and Padilla et al. [14,15] have reported the generation of fast and slow waves using finite-difference time-domain (FDTD) simulation. Haiat et al. have investigated the influence of trabeculae bone microstructure and material properties on QUS parameters using numerical simulations [16]. Our group has also tried to confirm the applicability of elastic FDTD method for the simulation of two-waves propagation in cancellous bone using three-dimensional X-ray CT images [17,18]. In these studies, we have reported the accordance between the FDTD simulation and experimental results. We also confirmed that the simulated peak amplitudes ratio of fast and slow waves showed accordance with the experimental results. Since the positions and conditions of sound source or receivers are easy to be changed in simulation, the FDTD analysis of wave propagation using actual CT data is useful not only for understanding the behavior of sound wave but also for an optimal design of a new diagnostic system.

In this two-wave propagation phenomenon, the fast wave mainly propagates in trabeculae and reflects its structure [17–19]. This means that the fast wave provides information on the trabeculae structure. In this study, therefore, by simulating the fast wave propagation in the cancellous bone, we especially aimed at clarifying the mechanism of fast wave generation focusing on the attenuation. We also checked the adequacy of the simulated results by comparing them to experimental results using actual bone samples.

2. Elastic FDTD method

The followings are the governing equations of three-dimensional elastic FDTD method for the isotropic medium related to x direction

$$\frac{\partial \sigma_{xx}}{\partial t} = (\lambda + 2\mu)\frac{\partial v_x}{\partial x} + \lambda\frac{\partial v_y}{\partial y} + \lambda\frac{\partial v_z}{\partial z}, \tag{1}$$

$$\frac{\partial \sigma_{xy}}{\partial t} = \mu\left(\frac{\partial v_x}{\partial y} + \frac{\partial v_y}{\partial x}\right), \tag{2}$$

$$\frac{\partial v_x}{\partial t} = \frac{1}{\rho}\left(\frac{\partial \sigma_{xx}}{\partial x} + \frac{\partial \sigma_{xy}}{\partial y} + \frac{\partial \sigma_{zx}}{\partial z}\right), \tag{3}$$

where σ_{ij} is normal and shear stresses, v_i is particle velocity, λ and μ are Lame's coefficients, ρ is density of the medium. In this simulation, the elastic anisotropy in the solid part was not considered. Using the same equations for y and z directions, the stress and particle velocity were calculated alternately both in the spatial and time-domains, which was called 'leapfrog method' [20]. Here, the absorption in both media was not introduced, however, it was confirmed by our group that the amplitude ratio of fast wave and slow wave was in good agreement with the experimental results [5–6].

3. Simulation model and measurement system

3.1. FDTD simulation model

For FDTD simulation, three parallelepipedic bovine cancellous bone samples A, B and C were used. The size of three samples used were 15 × 15 × 9–12 mm. Fig. 1a and b are the examples of X-ray micro focus CT images (SMX-100CT, SHIMADZU, Kyoto, Japan). The samples were obtained from the femoral head of 36 months old bovine. Spatial resolution of the CT images was 46 μm. Here, the resolution of the CT model of human cancellous bone used by Haiat et al. was 30 μm [21]. The mean thickness of bovine cancellous bones is larger than human bones. The reported mean thickness of human trabeculae is from 50–150 μm [22], whereas that ob bovine bone is from 150–200 μm. Therefore, the spatial resolution of our simulation model seems reasonable. The value at each point in the CT images was binarized in order to separate the ambiguous border between solid parts (trabeculae) and liquid parts with a specific threshold. The threshold was decided as the median value of the grayscale tones of the image.

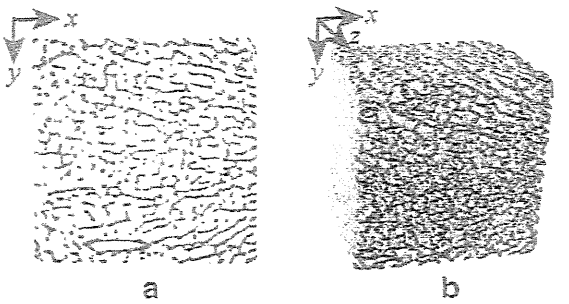

Fig. 1. An X-ray CT image of bovine sample used in numerical simulation. (a) Two-dimensional X-ray CT image of sample B. (b) Three-dimensional X-ray CT image of sample B.

The total simulation field was 17 × 17 × 13 mm with cube lattice of 46 μm. This is the maximum size for our computer memory (4GB). Time step was 4 ns. As the initial particle velocity at the surface of the plane source shown in Fig. 2. The initial waveform comes from the experimentally observed waveform of a single sinusoidal sound wave at 1 MHz that passed through the water. In order to avoid the strong instabilities of the simulation, the waveform was treated with low-pass filter whose cut-off frequency was 10 MHz. The filtered waveform is shown in Fig. 3. In this model, the bone sample was fully immersed in water.

As the speed of longitudinal wave in the solid part of the cancellous bone, the experimentally observed values of bovine cortical bone in the MHz range were used [23–26]. The speed of the shear wave was an estimated value, assuming the Poisson's ratio of 0.35. The parameters used in this simulation are shown in Table 1. The FDTD simulation software was originally programmed by our group [27].

In the first simulation, the wave propagated from the top to bottom surfaces. The propagating direction is parallel to the bone

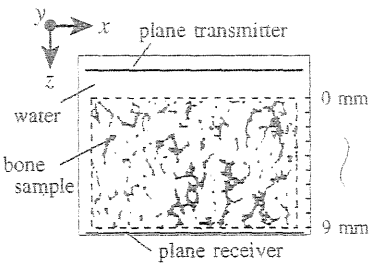

Fig. 2. Simulation model. A plane transmitter faces towards the sample immersed in water.

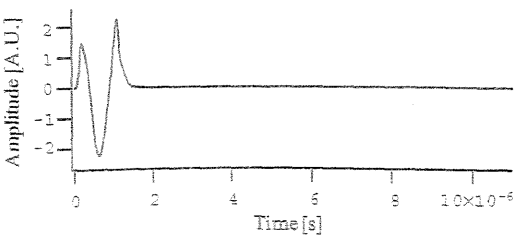

Fig. 3. Initial particle velocity.

Table 1
Parameters used in the FDTD simulation

Material		Water	Bone trabecula
Density [10^3kg/m^3]		1.0	2.0
Velocity [m/s]	Longitudinal	1500	3500
	Shear	-	2400

axes. In order to evaluate the attenuation of propagating waves in bone, the sample was virtually ground gradually from the bottom surfaces. The samples were shorten gradually from 9 to 1 mm thickness with an interval of 1 mm. Using the sample of smaller thickness, the simulation was performed again. By comparing the amplitudes of the first peak of calculated waveforms obtained at each thickness, the spatial distribution of the attenuation in the sample was obtained. The attenuation value a is calculated by the following equation:

$$a = \frac{20\log(V_n/V_{n+1})}{\Delta x}, \quad (4)$$

where V_n is the first peak amplitude of fast wave when the thickness of specimen is n mm, Δx is thickness difference between the measurements.

In the second simulation, the wave propagated from the bottom to top surfaces. We also obtained the spatial distribution of attenuation by filing away the sample from the top surface.

3.2. Measurement system for experiments

The attenuation measurements were also performed experimentally. The size of bone samples was 20 × 20 × 15 mm. The samples were obtained from the same part in the femoral head of 36 months old bovine. During measurements, the bone sample was immersed in degassed water in an acoustical tube at room temperature. The surface area of the plane PVDF transmitter and receiver (self-made, using PVDF films) were 20 × 20 mm. This comparatively large transducer brings good signal to noise ratio of the observed waves. The distance between two transducers was 60 mm.

A single sinusoidal wave at 1 MHz, with amplitude of 5 V_{p-p} (peak to peak voltage) from a function generator (WF1945, NF Corporation, Kanagawa, Japan) was amplified 20 dB by a power amplifier (4055, NF Corporation, Kanagawa, Japan), and applied to the transmitter. The waves that passed through the sample from top to bottom surfaces were investigated by a digital oscilloscope (TDS 524A, Tektronix Inc., Oregon, United States) with 40 dB preamplifier (5307, NF Corporation, Kanagawa, Japan). The propagating direction was parallel to the bone axes.

Similar to the FDTD studies, the thickness of actual specimens was filed away from the bottom surface. The measurements were done using samples changing thickness from 15 to 6 mm.

4. Results and discussion

4.1. Numerical results

Some examples of simulated waveforms are shown in Fig. 4. Fig. 4a shows the result when the wave passed through reference water alone. The small fluctuation in the wave tail comes from the instability of simulation, mainly due to the high-frequency component of the initial waveform. The fluctuation, however, was never observed in the area of fast wave. Fig. 4b shows the result when the sample was 9 mm thick and c shows the result of the sample 5 mm thick. In both waveforms of Fig. 4b and c, fast and slow waves can be seen. The amplitudes of the fast waves were always much smaller than those of the slow waves, which has also been reported in the experimental studies [5–7]. From the peak amplitudes of fast waves, the distribution of attenuation [dB/mm] can be evaluated; e.g. using peak amplitudes of 9 mm thick and 8 mm thick, we obtained the distribution of attenuation values between the positions of 8 to 9 mm from the surface.

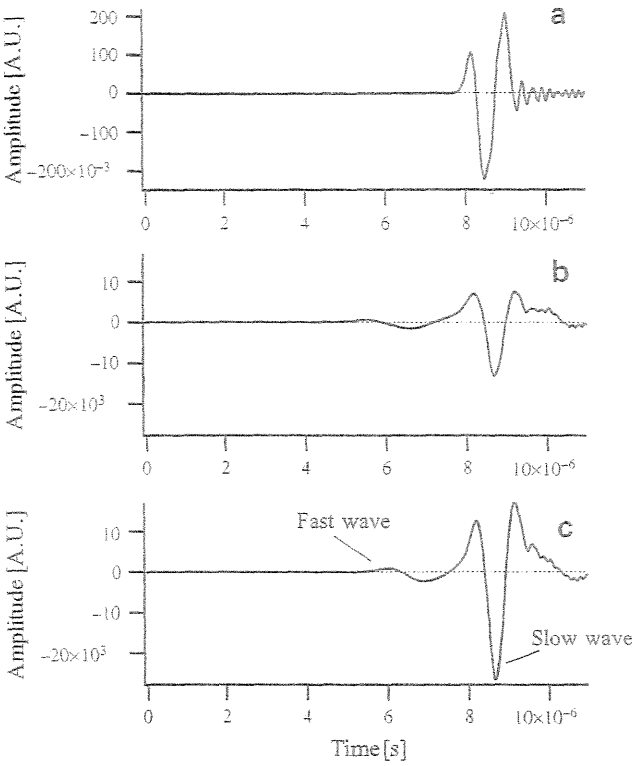

Fig. 4. Numerically simulated waveforms. (a) Without sample. (b) With sample of 9 mm thick. (c) With sample of 5 mm thick.

The distribution of BV/TV (bone volume/total volume) and fast wave attenuation of three specimens are shown in Figs. 5 and 6. The BV/TV was obtained from each 1 mm slice of three-dimensional model of bone constructed by CT data. The area of solid part was numerically examined in each slice. Fig. 6a shows the results when the wave propagated from top surface and b shows the results from the bottom surface. Here, the values of horizontal position axis mean the observed position from the top surface. These data show that the attenuation of fast wave is always higher in the early state of propagation. As the wave propagates in the bone, the attenuation gradually decreased and became almost constant.

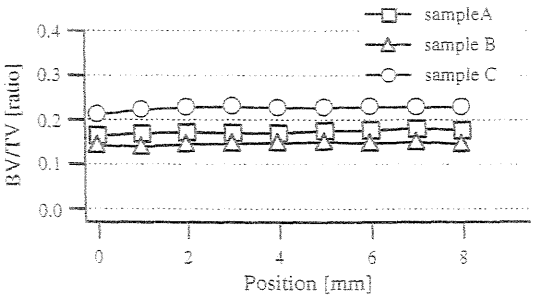

Fig. 5. Distributions of bone volume fraction of tree samples used in simulation.